www.czasopisma.pan.pl PAN POLSKA AKADEMIA NAUK www.journals.pan.pl

Arch. Metall. Mater. **66** (2021), 1, 127-134

DOI: 10.24425/amm.2021.134768

XIAOMING LI[1,2], YI LI[1], XIANGDONG XING[1,2*], YANJUN WANG[1], ZHENYU WEN[1], HAIBO YANG[1]

EFFECT OF PARTICLE SIZES OF SLAG ON REDUCTION CHARACTERISTICS OF NICKEL SLAG-COAL COMPOSITE BRIQUETTE

Nickel slag has a high-content iron and is a secondary utilization resource with great development potential. The coal-based direct reduction is an innovative technology that can be used to utilize the iron resources in nickel slag. The effect of the particle size of nickel slag on the strength and the reduction of nickel slag-coal composite briquettes were investigated. Four samples with particle size of 75~106 μm, 106~150 μm, 150~270 μm, and >270 μm were selected. The drop strength increased 9.4 times and the compressive strength reached 281.1 N when the nickel slag particle size decreased from >270 μm to 75~106 μm. The reduction degree determined by the data from the thermogravimetric experiment indicated that its maximum was 79.545%. The reduction experiments performed at 1200°C for 45 minutes indicated that the nickel slag with particle sizes between 75~106 μm were appropriate for the reduction of the nickel slag-coal composite briquettes.

Keywords: resources reutilization, nickel slag, particle size, direct reduction, reduction characteristics

1. Introduction

Nickel slag is a by-product of the flash furnace or the oxygen-rich top-blowing furnace nickel smelting process [1]. At present, the storage of nickel slag in China reaches 40 Mt and increases about 2 Mt per year [2]. However, a large amount of nickel slag is still treated by stockpiling, which not only takes up land, but also wastes potential metal resources. Nickel slag contains about 40% iron which is an available secondary metallurgical resource and its high iron content should be addressed and recycled. Nevertheless, the iron in nickel slag is in the form of fayalite, which is difficult to reduce.

Many technologies or processes have been developed to recover iron element from nickel slag [3-6]. Melting reduction requires more energy and consumes more resources than direct reduction, which can reduce the iron in nickel slag by reducing agent for subsequent magnetic separation. After deep reduction and magnetic separation of nickel slag, the iron concentrate grade was close to 90% and the recovery rate was more than 93% [3]. The direct reduction process has attracted attention from researchers due to its low temperature, stable process technology and simple operation. This technical of disposing waste nickel slag is not only economic, more importantly, with environmentally friendly.

There are many direct reduction processes, each has different process parameters, but most of the raw material is made into briquettes to facilitate the reaction. The particle size of the raw material is an important factor affecting the reduction of the briquettes. Previous studies have shown that the particle size has an important influence on the strength and the reduction [7,8], the reduction kinetics [9-12] of iron ore-coal composite briquettes, and the rates of the MnO reduction [13]. However, few studies had been done on the effect of particle size of nickel slag during coal-based reduction.

To determine the appropriate particle size of the nickel slag for producing composite briquettes, the effect of the particle size on nickel slag reduction and the reduction characteristics of composite briquettes were studied. It provides a theoretical basis for the reduction and iron extraction of nickel slag to a greater extent.

2. Experimental

2.1. Materials

The nickel slag samples, which contained 39.40 mass% Fe, 0.455 mass% Ni, 32.50 mass% SiO_2 and 9.70 mass% MgO, were

[1] XI'AN UNIVERSITY OF ARCHITECTURE AND TECHNOLOGY, SCHOOL OF METALLURGICAL ENGINEERING, XI'AN 710055, P.R. CHINA
[2] SHAANXI ENGINEERING RESEARCH CENTER OF METALLURGICAL, XI'AN 710055, P.R. CHINA

* Correspondence address: xaxingxiangdong@163.com

collected from a plant in China. The chemical compositions of the nickel slag are shown in Table 1.

TABLE 1

Chemical composition of the nickel slag (mass fraction, %)

TFe	FeO	SiO_2	MgO	CaO	Ni	Cu	Co	S
39.40	50.66	32.50	9.70	1.20	0.455	0.338	0.144	0.868

The X-ray diffraction pattern shown in Fig. 1 confirmed that the three major minerals in the nickel slag were fayalite (Fe_2SiO_4), magnesium silicate (Mg_2SiO_4), and iron-nickel sulfide ($FeNiS_2$).

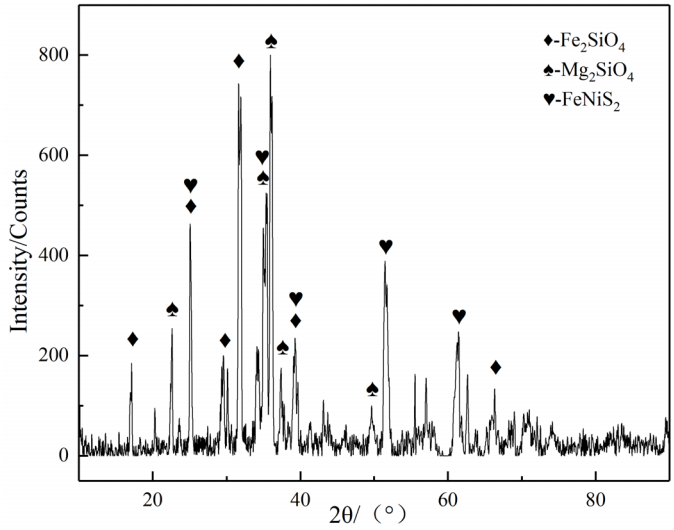

Fig. 1. X-ray diffraction pattern of the nickel slag

The element distribution is shown in Fig. 2. O, Si, and Fe were uniformly distributed. Si and Fe appeared in the same region, meaning the silicon was in the form of fayalite, which was consistent with the XRD results.

Coal with high fixed carbon and low ash content was used as a reductant in this study. Its industrial analysis results are listed in Table 2. The particle size of coal is less than 75 μm, and the adhesive in the compaction experiment is carboxymethyl cellulose powder with particle size less than 44 μm.

TABLE 2

Industrial analysis of the coal (mass fraction, %)

Moisture	Ash	Volatile	Fixed carbon	P	S
0.21	12.72	9.80	77.27	0.005	0.027

2.2. Experimental Procedure

The nickel slag was first crushed into four particle sizes: 75~106 μm, 106~150 μm, 150~270 μm, and >270 μm. The mixed samples were then prepared by mixing nickel slag, coal and adhesive (carboxymethyl cellulose) in a ratio of 1:0.15:0.01 with appropriate amounts of water (8%). The mixed samples were partly used to determine the reduction degree and the reduction rate by thermogravimetric testing with a powder mixture. The remains were pressed into composite briquettes to determine the reduction characteristics of the nickel slag-coal composite briquette by the strength and reduction experiments.

The thermogravimetric tests were performed using a thermogravimetric analyzer (SETARAM, France). Approximately 5 mg of the powder sample was used for each experimental, and the sample was placed in a circular crucible with height of 8mm and diameter of 5 mm. The weight loss of the sample was recorded from room temperature to 1200°C and heat preservation with heating rates of 5°C/min, 10°C/min, 15°C/min, 20°C/min, respectively. To ensure reproducibility of the results, each test was repeated three times before the results were determined.

The composite briquettes (4-6 g with an almond shape (10×12×12 mm)), were produced by a laboratory scale twin-roller briquette machine and dried at 120°C for 4h in a drying

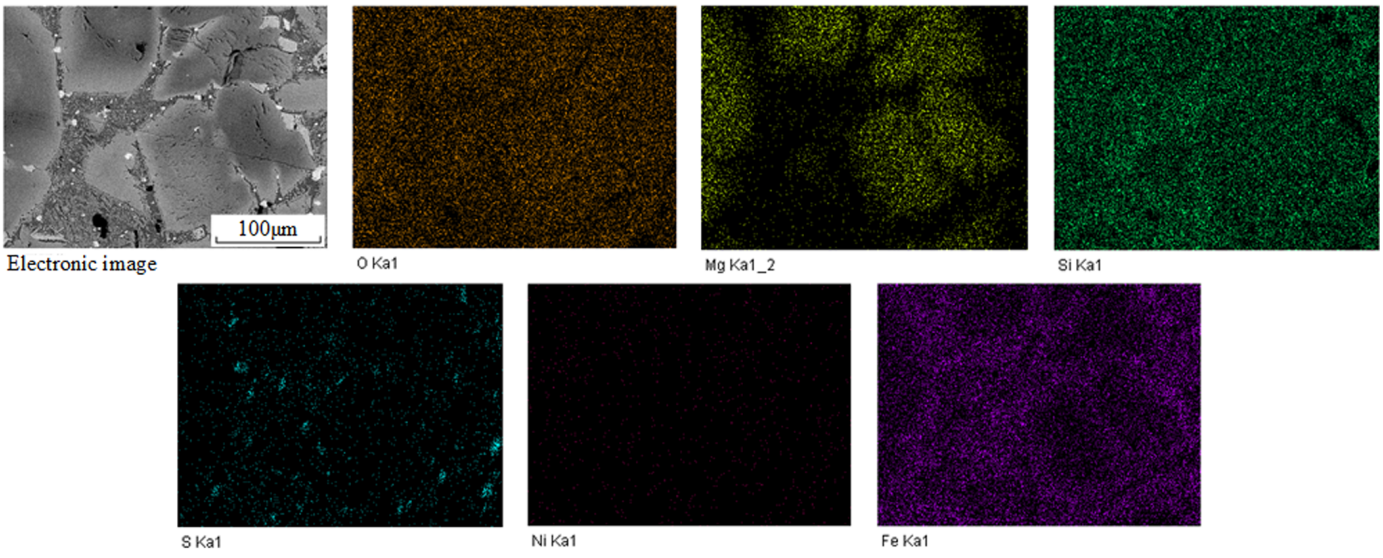

Fig. 2. Element distribution of the nickel slag

oven. Then the drop strength and the compressive strength of composite briquettes were measured. The drop strength was measured by dropping five composite briquettes individually from a height of 500 mm onto a 10 mm-thick steel plate until they broke. The final value was taken as the average of the five test values. The compressive strength was measured by a strength-testing instrument. The final value was calculated as the arithmetic mean of the five test values.

The reduction experiment of composite briquettes was performed using the device shown in Fig. 3, including a vertical high-temperature furnace, a transformer, a PID programmable temperature controller, and a thermocouple. A piece of the composite briquette was placed into a corundum crucible and reduced in the vertical furnace at 1200°C for 45 minutes. It was then slowly cooled in a container to room temperature under a nitrogen atmosphere.

The crystalline phases of the residues after reduction were identified by X-ray diffraction (XRD) (PANalytical, Netherlands) using Cu-Kα radiation, at 40 kV, 40 mA, a scan speed of 4°/min, with a step of 0.026°. The JADE software was used to analyze the unit cell parameters with the XRD results. The morphology of the samples was characterized by scanning electron microscope (SEM) (Phenom-World, Netherlands) equipped with an energy-dispersive spectrometer (EDS) at an acceleration voltage of 15 kV.

2.3. Thermodynamic Basis for Reduction

The carbothermal reduction products of the nickel slag was obtained via HSC Chemistry, which is a database software commonly used in the field of thermodynamics. The Equilibrium Com-positions module was primarily used during the calculation process.

During the calculation, the temperature was set to 1200°C, and the system pressure was 101325 Pa. The calculation result is shown in Fig. 4. Main reactions and standard Gibbs free energies are shown in Table 3.

The phase equilibrium diagram of Fig. 4 shows that the mole fraction of the fayalite continued to decrease as the tem-

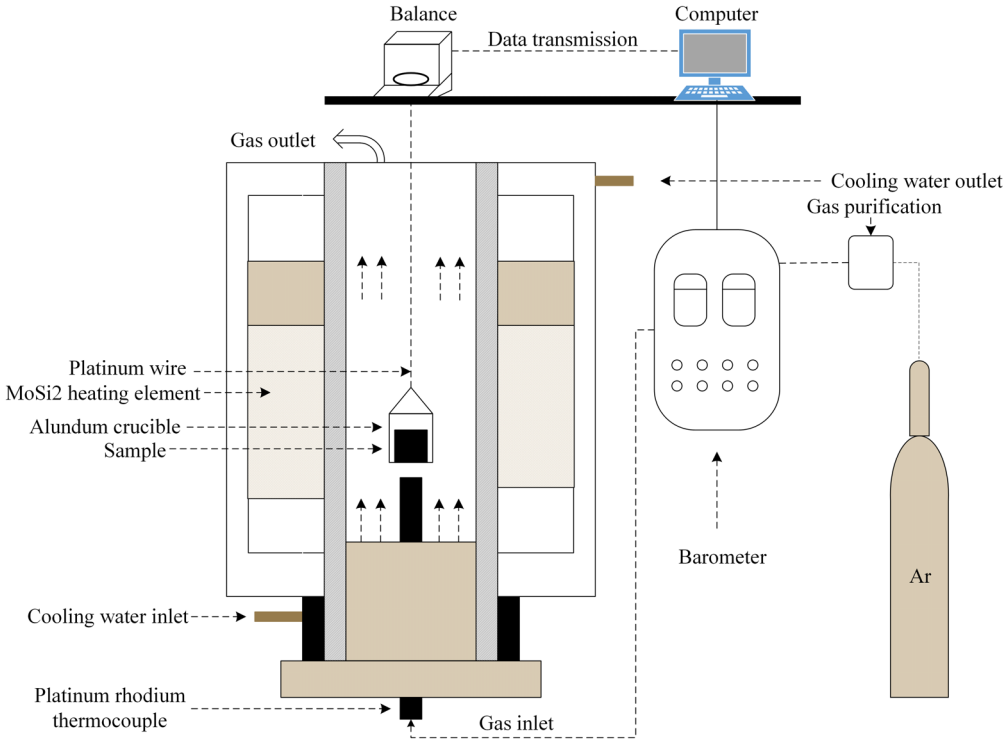

Fig. 3. Schematic diagram of the experimental device

TABLE 3

Main reactions and standard Gibbs free energies

No.	Reation	ΔGθ/(J·mol-1)	Tstart/°C
(1)	Fe2SiO4(s) + 2C(s) = 2Fe(s) + SiO2(s) + 2CO(g)	319421-299.85T	792.12
(2)	Fe2SiO4(s) + CaO(s) + 2C(s) = 2Fe(s) + CaSiO3(s) + 2CO(g)	241859-317.94T	487.56
(3)	FeO(s) + C(s) = Fe(s) + CO(g)	111619-154.95T	447.21
(4)	FeO(s) + CO(g) = Fe(s) + CO2(g)	16950-20.64T	548.22
(5)	C + CO2 = 2CO	123849-176.16T	429.90
(6)	CuO(s) + C(s) = Cu(s) + CO(g)	37509-71.35T	–54.09
(7)	NiO(s) + C(s) = Ni(s) + CO(g)	121619-172.64T	431.46

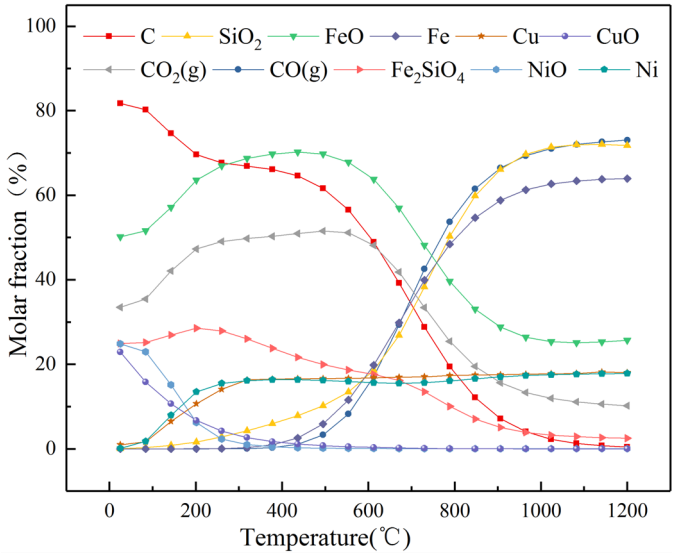

Fig. 4. Product compositions of nickel slag in different carbothermal reduction temperature

perature increased. At the temperature higher than 1100°C, the most common phases in the equilibrium were CO, Fe, and SiO_2, a rapid rise to become the main phase at a temperature slightly higher than 600°C. The main reason is that the fayalite ($2FeO \cdot SiO_2$) reactions with CaO or carbon occurred at this temperature [14]. The indirect reduction shown in Eq. (4) plays a dominant role [15].

A small amount of copper and nickel appeared due to the presence of the reaction (6) and (7), but they were not the dominate because of the lower content of copper and nickel oxides. Based on the thermodynamic calculation, it seems feasible to recover metallic from nickel slag with coal-based directly reduction.

3. Results and Discussion

3.1. Effect of Particle Size on the Strength of Nickel Slag-Coal Composite Briquettes

The effect of the particle size of nickel slag on the strength of the composite briquettes are presented in Table 4. The particle size influenced the strength of composite briquettes, including both the drop strength and the compressive strength. When the nickel slag particle size decreased from >270 μm to 75~106 μm, the drop strength of the composite briquette increased 3.2 times and the compressive strength reached 151.2 N per briquette. The small interparticle pores made the contact tight and the original cohesive force large. The decreased particle size resulted in an increased compaction and a higher strength of the briquette.

TABLE 4

Effect of particle size on the strength of composite briquettes

Particle size of nickel slag (μm)	Drop strength (numbers)	Compressive strength (N per briquette)
>270	3.2	30.7
150~270	5.0	94.4
106~150	6.0	110.9
75~106	6.4	151.2

3.2. Effect of Nickel Slag Particle Size on the Reduction Degree

The weight loss of the samples was continuously measured using a thermogravimetric analyzer and the lost weight was converted into the reduction degree (α_t) using the following equation [16]:

$$\alpha_t = \frac{m_0 - m_t}{m_0} \tag{8}$$

where m_0 is initial weight of samples and m_t is the weight of samples at temperature t.

The reduction degree of nickel slag with the particle size during the non-isothermal ran at a heating rate of 20°C/min up to 1200°C, see Fig. 5. At around 500°C, the reduction degree of the four particle sizes began to increase, so the reduction began around this temperature. As the temperature increased, the reduction degree increased for the all mixtures. The reduction degree of nickel slag with particle size of 75-106 μm was the highest under the same reduction time, which could achieve 79.545%. The change of reduction degree was mainly caused by the reduction of iron oxide, and the reduction of nickel oxide and copper oxide has small contribution because of its low content in the nickel slag. Maximum reduction degree is about 80%, because nickel slag is low in melting point while high temperature promotes reduction. However, at high temperature the slag can easily melt and the gas diffusion is limited, which deteriorates the kinetic conditions of gas-solid reaction, and inhibit the reduction process. In the process of coal-based reduction, the carbon in coal mainly reacts with iron olivine in nickel slag. When the

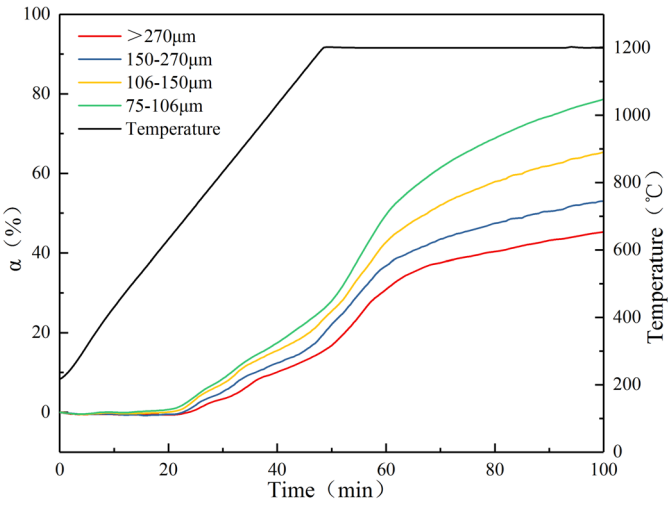

Fig. 5. Reduction degree of nickel slag with different particle sizes during the heating to 1200°C

particle is small in size, the contact area between the reductant and nickel slag is large, and it is easier to make reduction happen. After reduction, the gaps in nickel slag leads to increased surface roughness, and larger specific surface, which are more conducive to the reaction.

Reduction degree of the same particle size (106-150 μm) at various heating rates are shown in Fig. 6. The dotted line in Figure 6 is the heating curve at different heating rates and their initial temperatures are all 600°C, which are heated to 1200°C and then remain. The intersection point of dotted line and solid line in the same color is the reduction degree of the mass when the temperature reaches 1200°C. The particle size of 106-150 μm was selected considering the industrial application, as the energy consumption was lower when crushing. When the heating rate was 5°C/min, the reduction degree reached a maximum of 73.2%. As the heating rate increased, the final reduction degree gradually increased. When the heating rate was lower, the reaction time was longer, and the reaction was more complete. At the heating rates of 5°C/min, 10°C/min, 15°C/min, and 20°C/min (up to 1200°C), the corresponding reduction degree was 34.413%, 32.224%, 31.773%, and 30.079% respectively.

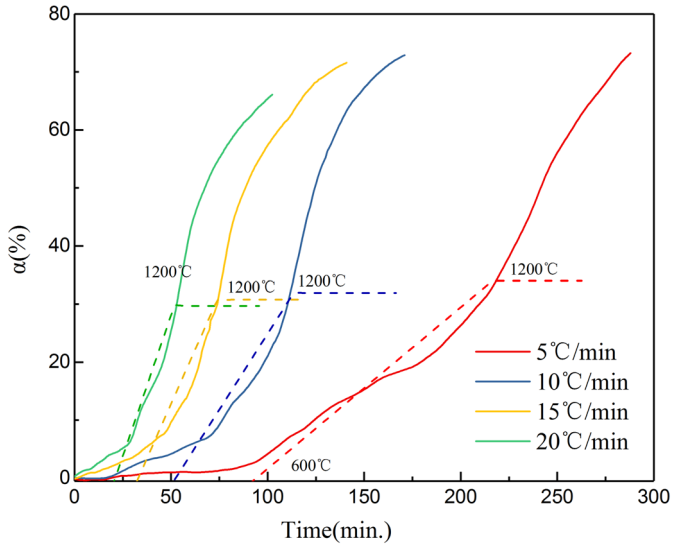

Fig. 6. Reduction degree of nickel slag with particle sizes between 106-150 μm at different heating rates

3.3. Effect of Nickel Slag Particle Size on the Reduction Rate

The derivative thermogravimetry curves with various particle sizes are shown in Fig. 7. The change of particle size caused the change of the initial reaction temperature and the reduction rate. The curves corresponding to the four particle sizes exhibited a similar change trend. The smaller the particle size, the greater the weight loss rate at the same time. When the particle size changed from >270 μm to 75~106 μm, the maximum reduction rate increased from –0.37%/min to –0.51/min. The reduction rate of samples with the average particle size of 75~106 μm was higher than the other particle rates. The reduction rate decreased as the particle size increased, in accordance to the unreacted-core mode [17], so it took additional time for the nickel slag to obtain a larger particle size and reach the same metal rate. The increased nickel slag size led to the reduced contact area of the fayalite and the coal, which was not conducive to their reduction. The lower particle size signified the bigger contact surface area, which led to additional reduction of iron oxide, thus increasing the reduction degree of the nickel slag.

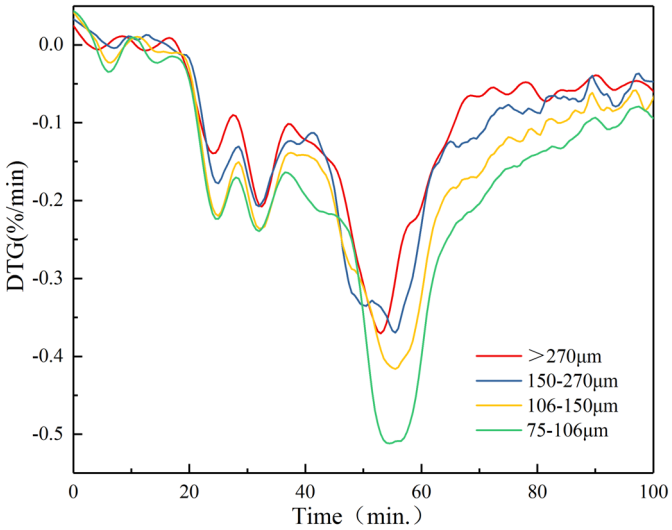

Fig. 7. Derivative thermogravimetry of four particle size mixtures during the heating up to 1200°C

Derivative thermogravimetry curves of the same particle size (106-150 μm) at various heating rates are shown in Fig. 8. The temperature of maximum DTG is 1201°C, 1154°C, 1150°C and 1102°C when the heating rate is 5°C/min, 10°C/min, 15°C/min and 20°C/min, respectively. With the increase of the heating rate, the corresponding temperature for DTG to reach its peak value varies greatly, which is related to the volatile content in raw materials. The higher the volatile content, the smaller the

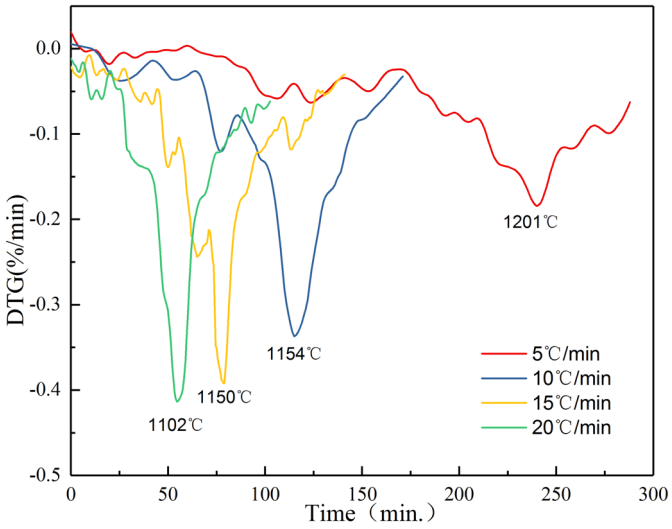

Fig. 8. Derivative thermogravimetry of different heating rates during the heating up to 1200°C

influence of heating rate on the high temperature reaction, and vice versa. When the heating rate was quicker, the temperature where the peak weight loss rate was reached decreased. Decreasing the heating rate was beneficial to the reduction reaction [18]. Reducing the heating rate is conducive to the reduction reaction because at the same temperature, it takes a longer time at a smaller heating rate, leading to a more thorough reaction. As the reaction between iron oxide and reductant prolongs, the reduction degree increases with the decrease of the heating rate.

3.4. The Characterization of the Reduction Products

The degree of metallization of the products with coal-based direct reduction of nickel slag is shown in figure 9. At a certain temperature, with the extension of the reduction time, the metallization rate first increases, then tends to be stable, and finally reaches about 85%. Therefore, the iron oxide in nickel slag can be reduced to a large extent by coal-based direct reduction.

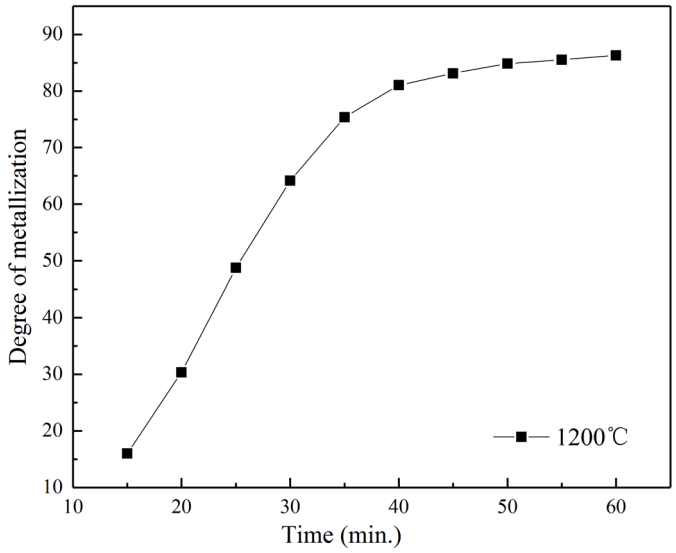

Fig. 9. The degree of metallization of nickel slag direct reduction

The phase composition of the reduction products investigated by X-ray diffraction analysis is shown in Fig. 10. The reduced product was primarily metallic iron, the copper and nickel were not detected because of the lower content of copper and nickel oxide in the nickel slag. If they are reduced, they must dissolve in metallic Fe. The higher peak of metal iron signified the higher reduction degree. The nickel slag with particle size greater than 270 μm had small quantities of metallic iron after the reduction indicted that the nickel slag could not be reduced completely in this particle size. As the nickel slag particle size decreased to 150~270 μm, the peak characteristics of the metallic iron phases increased, while the peak characteristics for fayalite (Fe_2SiO_4) decreased. When the nickel slag particle size decreased to 75~106 μm, the reduction of the nickel slag became more complete.

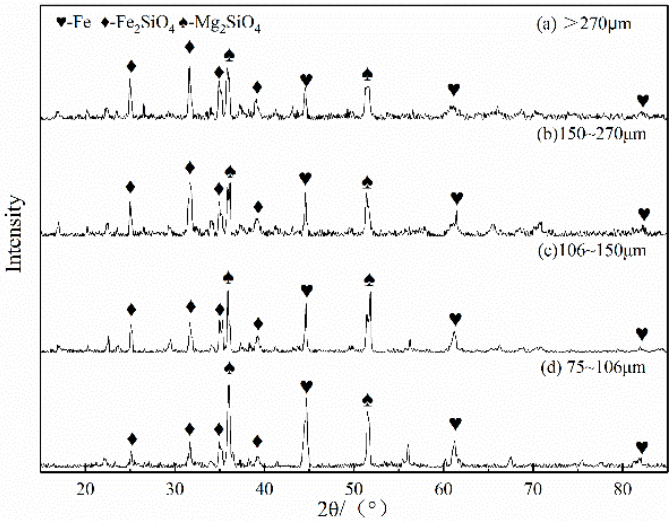

Fig. 10. X-ray diffraction patterns of reduction products with different particle size at 1100°

The computational tolerances were present from Table 5 for each parameter. It shows that a concomitant change in crystallographic parameters was observed with the increase of reduction temperature. During reduction, the crystallographic parameters of fayalite gave a decrease in a and c from 4.8183 A and 6.0272A to 4.8279 A and 5.9218 A, respectively, corresponding to a decrease in unit cell volume from 303.87A^3 to309.71 A^3. It can therefore be inferred that with an increase in reduction temperature, the lattice of fayalite gradually shrank along both the a-axis and the c-axis, expand along the b-axis.

TABLE 5

Unit-cell dimension and volume of nickel slag heated in nitrogen atmosphere

Temperature	a/A	±	b/B	±	c/C	±	Volume/A^3
Raw	4.8176	0.0008	10.3279	0.0007	6.0220	0.0004	303.15
500°C	4.8083	0.0013	10.3281	0.0009	6.0272	0.0003	303.07
600°C	4.8076	0.0009	10.3297	0.0011	6.0102	0.0007	302.23
700°C	4.8009	0.0011	10.3350	0.0004	6.0013	0.0003	301.92
800°C	4.7822	0.0005	10.3391	0.0008	5.9891	0.0009	300.59
900°C	4.7801	0.0009	10.3428	0.0005	5.9732	0.0006	300.01
1000°C	4.7737	0.0007	10.3477	0.0003	5.9506	0.0005	299.89
1100°C	4.7705	0.0008	10.4373	0.0006	5.9489	0.0010	298.02
1200°C	4.7682	0.0010	10.5019	0.0011	5.9362	0.0005	297.71

The SEM images of the reduction products are shown in Fig. 11 and the EDS analysis of the points in figure 11 are listed in Table 6. EDS analysis shows the bright white shape in the SEM image is iron, and the gray part is slag phase containing elements Fe, Mg, O and Si. It can be intuitively seen from the picture that with the change of temperature and particle size, the final reduced iron shows different sizes. Fig. 11a shows the SEM images of the nickel slag with a particle size greater than

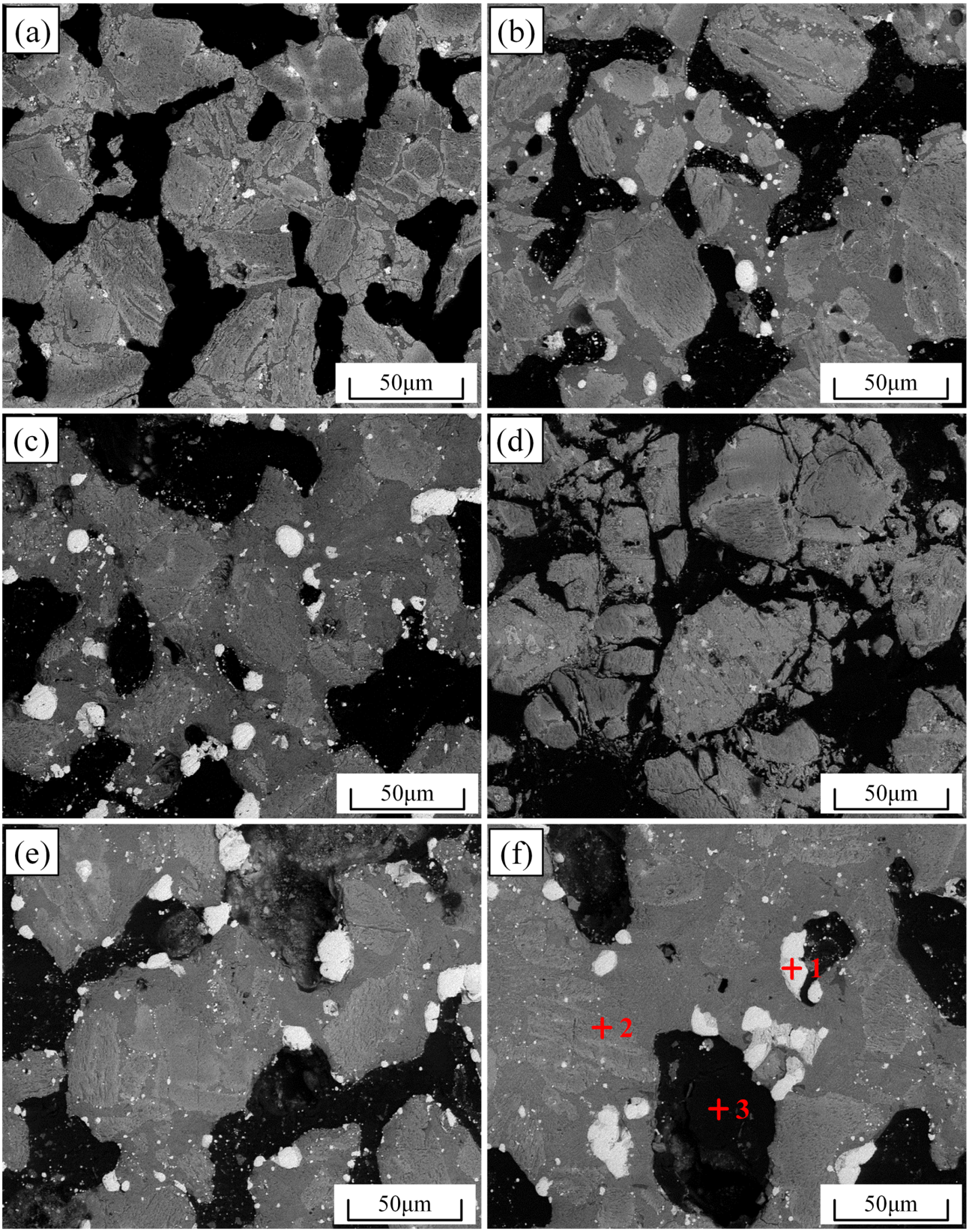

Fig. 11. Scanning electron micrographs of reduction products. a Nickel slag (>270 μm) at 1100°C; b nickel slag (150~270 μm) at 1100°C; c nickel slag (106~150 μm) at 1100°C; d nickel slag (75~106 μm) at 800°C; e nickel slag (75~106 μm) at 1100°C; f nickel slag (75~106 μm) at 1200°C

270 μm heated to 1100°C. The metallic iron particles (bright white) appeared in the periphery of the briquette and the gangues were partially sintered.

Fig. 11b, 11c, and 11e demonstrate that when the particle size of the nickel slag decreased from 150~270 μm to 75~106 μm, the microstructures of the briquettes were similar. There were large numbers of metallic iron in the observed area and the size of the iron particle was coarser as the nickel slag particle size decreased. The coarsening of metallic iron particles improved the liberation of metallic iron and gangue, which increased the iron content during the direct reduction.

Fig. 11d-f show the microstructures of the reduction products at 800°C, 1100°C, and 1200°C. The increased temperature enhanced the reduction of the nickel slag, so the quantity of metallic iron rose and the degree of aggregation grew. The temperature must be maintained above 1200°C in order to maximize the recovery of the metallic iron from the nickel slag.

TABLE 6

The chemical composition of the points in Fig. 10

Element	Point 1		Point 2		Point 3	
	Mass (%)	Atomic mass (%)	Mass (%)	Atomic mass (%)	Mass (%)	Atomic mass (%)
C-K			69.15	74.91	1.48	6.54
O-K	35.69	60.37	30.85	25.09		
Fe-K	47.37	22.96			98.52	93.46
Mg-K	2.28	2.54				
Si-K	14.66	14.13				
Total	100.00		100.00		100.00	

4. Conclusions

1. Decreasing the particle size of the nickel slag could increase the strength of nickel slag-coal composite briquettes and the reduction degree of nickel slag. The drop strength increased 9.4 times and the compressive strength reached 281.1 N when the nickel slag particle size decreased from >270 μm to 75~106 μm. The nickel slag particle size between 75~106 μm was appropriate to complete the reduction, the maximum reduction degree was 79.545%.

2. The lower the heating rate, the higher the reduction degree. At the the heating rates of 5°C/min, 10°C/min, 15°C/min, and 20°C/min (up to 1200°C), the corresponding reduction degree for the nickel slag with same particle size (106-150 μm) was 34.413%, 32.224%, 31.773%, and 30.079% respectively.

3. It is a feasible process to recovery iron from nickel slag via the coal-based direct reduction. The smaller the particle size, the greater the weight loss rate at the same time. The reduction rate of samples with the average particle size of 75~106 μm was higher than the other particle rates. The optimized particles size was between 75~106 μm at 1200°C for 45 minutes.

Acknowledgement

We thank the National Natural Science Foundation of China (Nos. 51774 224, 51574189) for financial support for this research.

REFERENCES

[1] C.F. Zhang, H.X. Liu, D.L. Zhong, D.W. Zeng, Chin. J. of Nonferrous Met. **9**, 805-810 (1999).
[2] X.M. Li, M. Shen, C. Wang, Y.R. Cui, J.X. Zhao, Mater. Rev. **31**, 100-105 (2017).
[3] W. Ni, Y. Jia, F. Zheng, Z.J.Wang, M.J. Zheng, J. Univ. Sci. Technol. Beijing. **32**, 975-980 (2010).
[4] W. Ni, M.S. Ma, Y. L. Wang, Z.J. Wang, F.M. Liu, J. Univ. Sci. Technol. Beijing. **31**, 163-168 (2009).
[5] X.Y. Guo, Q.Q. Gong, W.T. Shi, D.Li, Q.H. Tian, J. Cent. South Univ. **43**, 2048-2053 (2012).
[6] K.H. Liu, S.M. Li, H. Li, Z.F. Cong, Energy Saving of Nonferrous Metallurgym **2**, 14-17 (2016).
[7] X.M. Qin, T.C. Sun, A.H. Zou, S. Cheng, M. Jiang, C.Y. Xu, J. Kou, X.P.Hu, Min. Metall. Eng. **31**, 95-99 (2011).
[8] W. Yu, T.C. Sun, Z.Z. Liu, J. Kou, C.Y. Xu, ISIJ International. **54**, 56-62 (2014).
[9] Y. Man, J.X. Feng, Q. Ge, F.J. Li, J. Che. Pharm. Res. 2484-2490 (2014).
[10] M. Anis, B.D. Makahanap, A. Manaf, Indonesian J. Mater. Sci. **13**, 30-33 (2011).
[11] J. M. Pang, P. M. Guo, P. Zhao, C.Z. Cao, D.W. Zhang, J. Iron Steel Res. Int. **16**, 07-11 (2009).
[12] V. K. Trujic, Z. D. Zivkovic, Mater. Trans. **39**, 1012-1016 (2007).
[13] J.R. Oliveira, E.A. Vieira, D.C.R. Espinosa, J.A.S. Tenorio, Mater. Trans. **52**, 1200-1205 (2011).
[14] T. Tokiaki, W. Katsuya, K. Jiro, Mem. Fac. Eng., Hokkaido Univ. **8**, 14-22 (1950).
[15] Y.S. Sun, P. Gao, Y.X. Han, D.Z. Ren, Ind. Eng. Chem. Res. **52**, 2323-2329 (2013).
[16] Y.S. Sun, Y.X. Han, P. Gao, X.C. Wei, G.F. Li, Int. J. Miner. Process. **143**, 87-97 (2015).
[17] R.J. Fruehan, Metall. Trans. **B 8**, 279-286 (1977).
[18] Y. Takyu, T. Murakami, S.H. Son, E. Kasai, ISIJ International **55**, 1188-1196 (2015).